The gas-liquid surface tension of argon: A reconciliation between experiment and simulation

Florent Goujon,[1,a)] Patrice Malfreyt,[1] and Dominic J. Tildesley[2]
[1]*ICCF, UMR CNRS 6296, Université Blaise Pascal, 63177 Aubière Cedex, France*
[2]*EPFL-CECAM, Batochime (BCH), CH-1015 Lausanne, Switzerland*

(Received 26 March 2014; accepted 16 June 2014; published online 30 June 2014)

We present a simulation of the liquid-vapor interface of argon with explicit inclusion of the three-body interactions. The three-body contributions to the surface tension are calculated using the Kirkwood-Buff approach. Monte Carlo calculations of the long-range corrections to the three-body contribution are calculated from the radial distribution function $g^{(2)}(z_1, \cos\theta_{12}, r_{12})$. Whereas the effective two-body potentials overestimate the surface tension by more than 15%, the inclusion of the three-body potential provides an excellent agreement with the experimental results for temperatures up to 15 K below the critical temperature. We conclude that the three-body interactions must be explicitly included in accurately modelling the surface tension of argon. © *2014 AIP Publishing LLC*. [http://dx.doi.org/10.1063/1.4885351]

I. INTRODUCTION

The success of molecular simulations in the quantitative prediction of thermodynamic properties of bulk liquid and interfacial systems has been achieved with the use of relatively simple effective potentials which model the van der Waals and electrostatic interactions. In most cases, the simulations use two-body Lennard-Jones site-site potentials and partial charges. These pair potentials have been shown to be successful in reproducing the temperature dependence of the surface tension of various organic liquids,[1–12] water,[13–15] and acid gases.[16–19]

Although, the surface tension, γ of the simple Lennard-Jones liquid was the first to be studied,[20] the agreement between the simulated surface tension and the experimental results for liquid argon is poor (see Fig. 1). The differences with experiment cannot be attributed to methodological problems such as finite size-effects, long range corrections, and the intrinsic accuracy of different routes to γ. These problems are now well-controlled.[19]

These deviations from experiments cannot be attributed to insufficient simulation time since longer molecular dynamics simulations using adapted long-range corrections for two-phase systems were performed[21] and led to the same deviations. Modified Lennard-Jones potentials such as truncated and shifted potentials have also been applied to the calculation of surface tension[22] and exhibit a slight underestimation of the surface tension compared with experiments at each temperature (see Fig. 1). This means that it is however possible to find some approximate two-body potential which fits the surface tension results. This kind of potential ignores the long-range correction of the surface tension through the truncation and shift of the potential. Unfortunately, this tells us nothing about the interaction at play in determining the experimental surface tension of liquid-gas interface of argon. The differences must be understood in terms of the inaccuracy of the potential model. Argon has a large atomic polarizability and the triple induced-dipole potential is likely to make a significant contribution to the surface tension.[23–25]

Three-body potentials have been used to successfully predict the coexisting liquid and gas densities of argon using Monte Carlo, molecular dynamics[27] and the Gibbs Ensemble Monte Carlo method.[24,28] The three-body energy can also be estimated by perturbation theory[25] in simulations using two-body potentials. However, to our knowledge no simulations, including three-body potentials, have been performed on argon involving an explicit interface, that would allow us to calculate the surface tension. Approximate theoretical approaches suggest that the inclusion of three-body interactions will lead to more accurate predictions of the surface tension.[20,29]

In this paper, we calculate the surface tension of argon by molecular simulation using the Monte Carlo method with a three-body potential. We show that an excellent agreement can be found with experimental data, providing that the long-range corrections are included with care and that a sufficiently large cut-off is used to avoid the need for the inclusion of the long-range correction to the potential energy at each step in the Markov Chain. In Sec. II, we describe the system and the different interaction potentials studied in this work. Section III summarizes our results: in Sec. III A, we discuss the effect of including the long-range corrections. We choose a cutoff value so that cutoff effects are negligible in order to avoid including the long-range correction to the energy in the Metropolis scheme. In Sec. III B, we compare the values obtained for coexisting densities and vapor pressure with experiments and previous simulation works, for all potentials. We present in Sec. III C the relations for the calculation of the three-body contribution to the surface tension and its long-range corrections. We compare the obtained values with experiments and reference simulations using effective two-body interactions. Finally, we conclude that the use of a three-body

a)Electronic mail: florent.goujon@univ-bpclermont.fr

 © 2014 AIP Publishing LLC

This article is copyrighted as indicated in the article. Reuse of AIP content is subject to the terms at: http://scitation.aip.org/termsconditions. Downloaded to IP: 194.214.132.176 On: Tue, 01 Jul 2014 07:05:24

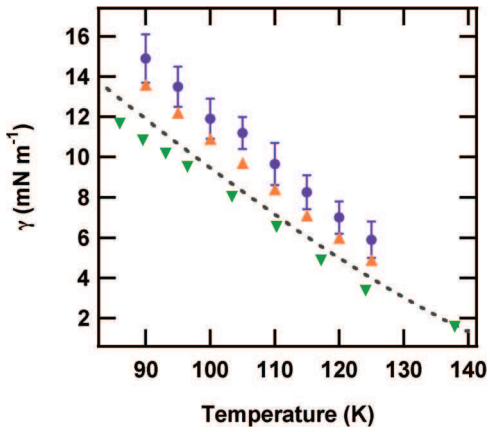

FIG. 1. Surface tension of argon as a function of the temperature: the dashed line is the experiment.[26] All the simulations results are for effective two-body potentials with additional long range corrections and γ is calculated using a variety of mechanical or thermodynamical approaches. Circles are Ref. 19, the inverted triangles are for the truncated and shifted potential of Ref. 22, the triangles are for the truncated and corrected potential with a more recent calculation of the long range corrections.[21]

potential as well as the calculation of long-range corrections are necessary to obtain accurate values for the surface tension of argon.

II. MODEL

An equilibrated liquid configuration is created using a simulation cell of $40 \times 40 \times 100\,\text{Å}^3$ containing $N = 3000$ argon atoms at the required temperature along the orthobaric curve and at a density close to the coexisting liquid density. Two additional empty simulation cells of $40 \times 40 \times 100\,\text{Å}^3$ are added to either side of the central cell in the z direction and periodic boundary conditions are applied to the final cell in the x, y, and z directions. Simulations are performed at constant-NVT using an equilibration phase of 3×10^5 Monte Carlo cycles (one MC cycle corresponds to N trials translational moves). The system forms two, stable liquid-vapor interfaces during the equilibration. During a further acquisition phase of 2×10^6 cycles, configurations are saved every 20 cycles. The cutoff radius for the two-body interactions, $r_{cut}^{(2B)}$, is set at 18 Å to avoid any dependency of the two body part of the surface tension on $r_{cut}^{(2B)}$. For the three-body interactions, the cutoff radius, $r_{cut}^{(3B)}$, must be lower than $L_x/4$ so that all the triplets are unique when using the minimum-image convention. In this work, $r_{cut}^{(3B)} = r_{cut}^{(2B)}/2 = 9$Å.

We performed three series of simulations using different interaction potentials: an effective two-body potential, the Lennard-Jones potential, used as a reference model. We used the parameters proposed by Vrabec[30] ($\epsilon = 116.79\,\text{K}$ and $\sigma = 3.3952\,\text{Å}$), since they provide an accurate prediction of the coexisting densities.

We have studied the following accurate two-body potentials, with an additional explicit three-body contribution: Barker-Fisher-Watts (BFW)[27] and a more recent potential obtained from accurate *ab initio* calculation by Nasrabad, Laghaei, and Deiters (NLD).[31] Analytical expressions for the BFW and NLD potentials can be found in Refs. 27 and 31, respectively.

The three-body interaction added to the accurate BFW and NLD potentials was the triple-dipole Axilrod-Teller[32] potential (AT),

$$v^{(3B)}(\mathbf{r}_i, \mathbf{r}_j, \mathbf{r}_k) = \frac{\nu(1 + 3\cos\theta_i \cos\theta_j \cos\theta_k)}{r_{ij}^3 r_{ik}^3 r_{jk}^3}, \quad (1)$$

where θ_i is the internal angle of the triangle, ijk centered on atom i. The AT parameter $\nu = 7.353 \times 10^{-90}$ J cm^9 is used throughout.

The two-body contribution to the surface tension is calculated using the mechanical definition of Kirkwood and Buff[33]

$$\gamma^{(2B)} = \frac{1}{2A}\left\langle \sum_i \sum_{j>i} \left[\frac{r_{ij}^2 - 3z_{ij}^2}{r_{ij}}\right] \frac{dv^{(2B)}}{dr_{ij}} \right\rangle \quad (2)$$

for an interface. Alternative approaches such as Irving-Kirkwood[34] and test-area[35] methods produce results for γ that agree with the Kirkwood-Buff approach to within the estimated simulation errors.[19]

III. RESULTS AND DISCUSSIONS

A. Size and cutoff effects

The simulated value of the surface tension can depend on the size of the cell, L_x along the surface. Small systems exhibit a significant oscillation in $\gamma(L_x)$.[36] The extent of the liquid phase in the z direction is also important, since local contribution to γ must be zero in the center of the cell. To avoid these size effects, we have used a system ($N = 3000$) in a simulation box cell of ca. ($11\sigma \times 11\sigma \times 28\sigma$). We will demonstrate that this cell is suitable for calculating the limiting value of the surface tension.

For a pair potential, it is possible to include the long range correction (LRC) for the potential energy explicitly in making the trial Monte Carlo move. The precise LRC for the energy of an atom i will depend on its position, z_i.[37–39] We have implemented the mean field method developed by Janeček,[38] which allows for the calculation of the density profile and γ in the presence of the long range field. We will compare this approach to the calculation of these properties in the same simulation without the Janeček correction. This will allow us to find the value of $r_{cut}^{(2B)}$ beyond which the Janeček correction can be safely ignored. This is important because it is complicated and difficult to apply this type of correction in the presence of a three-body interaction.

To this end, simulations using the Lennard-Jones potential[30] at $T = 90\,\text{K}$ with cutoff values ranging from $r_{cut}^{(2B)} = 8\,\text{Å}$ up to $r_{cut}^{(2B)} = 20\,\text{Å}$ were performed. Fig. 2 shows the liquid and vapor densities and the surface tension γ calculated for two models: the truncated Lennard-Jones (LJT) and truncated Lennard-Jones with the Janeček correction (LJT+JC). The values for the surface tension include the additional long range contribution to γ from distances beyond the cutoff. This can be calculated using the method described in Ref. 38 or by using the method of Blockhuis[40,41] for a sin-

This article is copyrighted as indicated in the article. Reuse of AIP content is subject to the terms at: http://scitation.aip.org/termsconditions. Downloaded to IP: 194.214.132.176 On: Tue, 01 Jul 2014 07:05:24

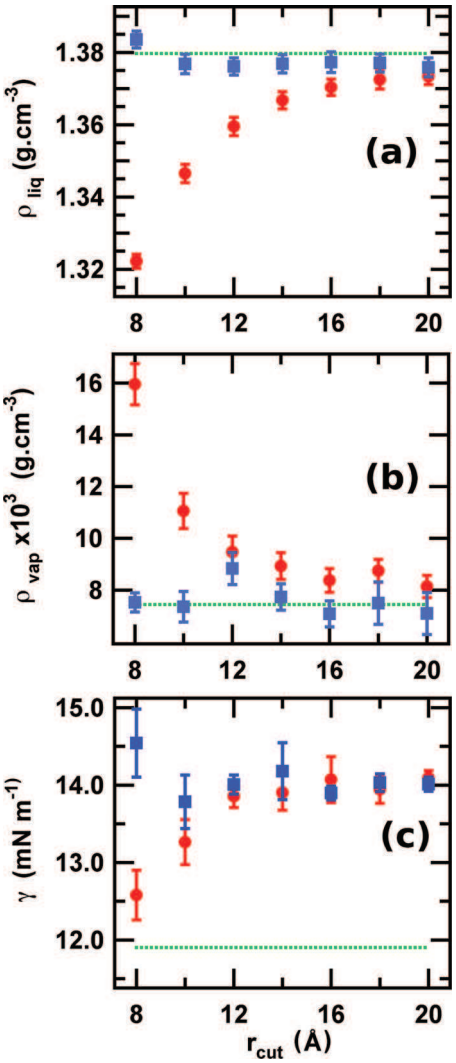

FIG. 2. (a) Liquid density, (b) vapor density, and (c) surface tension of argon as a function of the cutoff radius $r_{cut}^{(2B)}$ for the LJT model (circles) and the LJT + JC model (squares) at $T = 90$ K. The dotted lines represent the experimental values.[26] Note γ includes an additional LRC for both models. The error bar on γ is calculated from block average on the 100 000 saved configurations (five consecutive blocks of 20 000 configurations).

gle interface,

$$\gamma_{LRC}^{(2B)} = \frac{\pi}{4}\Delta\rho^2 \int_{-1}^{1} ds \int_{r_c^{(2B)}}^{+\infty} dr\, v^{(2)\prime}(r) r^4 (3s^3 - s) \coth\left(\frac{sr}{2\xi}\right), \quad (3)$$

where $\Delta\rho$ is the difference between liquid and vapor densities and ξ is the thickness of the interface. The error bar on γ is calculated by a block average on the 100 000 saved configurations (five consecutive blocks of 20 000 configurations).

These results are in good agreement with previous work.[21,38] In the case of LJT simulations, small values of the cutoff result in an underestimation of the coexisting liquid densities. The surface tension is also smaller for smaller cutoff values. LJT+JC model results in constant values regardless of $r_{cut}^{(2B)}$. Fig. 2(c) confirms that the overestimation of the surface tension is not due to cut-off effects: the limiting value is 15% higher than the experimental value in this case. It also demonstrates that we can avoid the Janeček correction at each step in Markov chain if we use a $r_c^{(2B)} = 18$ Å since the results for the LJT and the LJT+JC have the same limiting value at this point. This value of $r_c^{(2B)} = 18$ Å is used throughout the rest of this paper.

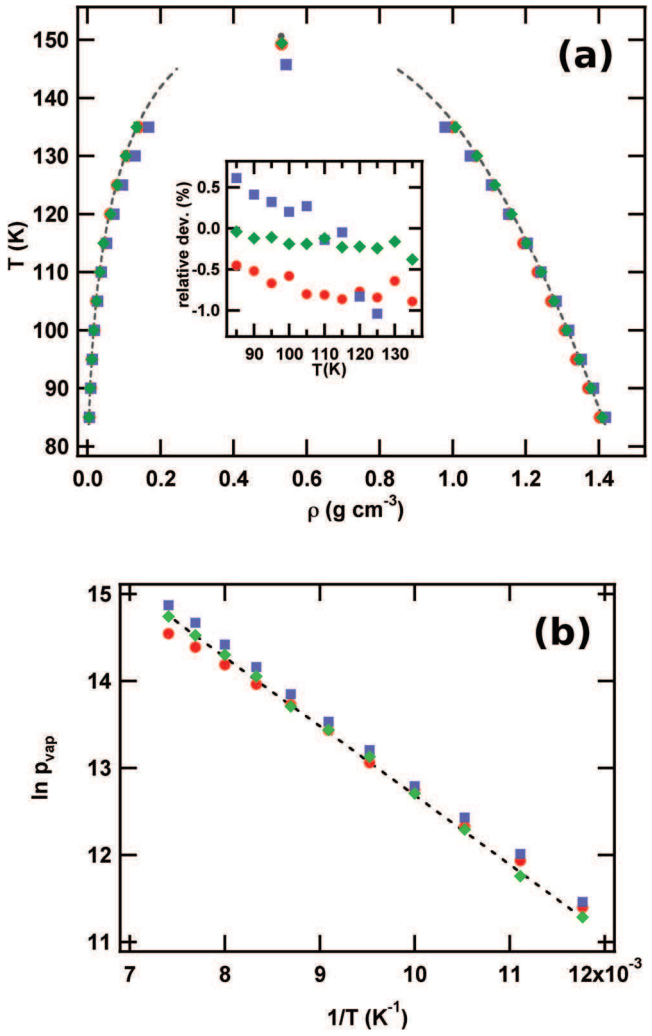

FIG. 3. (a) Phase diagram of argon calculated using • (red) effective two-body (LJ),[30] ■ (blue) (BFW + AT),[27] and ◆ (dark green) (NLD + AT)[31] potentials. The inset shows the relative deviation (%) of the liquid density from experiment for different temperatures. (b) Logarithmic vapor pressure as a function of inverse temperature. The dashed lines are experimental data.[26]

B. Coexisting densities

Fig. 3(a) shows the liquid-vapor coexisting densities calculated with LJ, BFW + AT, and NLD + AT potentials. The coexisting densities are calculated from the density profiles by averaging the density in the liquid and gas phases at distances greater than 20 Å from the Gibbs dividing surface. The error bars on the coexisting densities are smaller than the symbols in the figure.

The coexisting densities are accurately reproduced by all three sets of simulations: the relative deviation from experiment is less than 1% for LJ model, less than 3% for BFW + AT model, and less than 1% for NLD + AT model (see inset in Fig. 3(a)). The BFW + AT potential exhibits a slight deviation from the experimental curve at high temperature, predicting a critical temperature and density, estimated using

This article is copyrighted as indicated in the article. Reuse of AIP content is subject to the terms at: http://scitation.aip.org/termsconditions. Downloaded to IP: 194.214.132.176 On: Tue, 01 Jul 2014 07:05:24

the law of rectilinear diameters, that are 3% and 2% different from the experimental values. The LJT and NLD + AT models predict T_c within 1% and ρ_c within 0.3% of experiment. These results are in good agreement with similar studies using Monte Carlo simulations in the Gibbs Ensemble.[23,28] The inclusion of the three-body potential has little effect on these coexisting densities.

The vapor pressures p_{vap} for the three simulation sets are reported in Fig. 3(b) through $\ln p_{\text{vap}}$ (Pa) as a function of the inverse temperature. The calculation includes the kinetic, two-body and three-body contributions as well as the corresponding long-range corrections. Whereas the BFW + AT potential overestimates the vapor pressure, the LJT and NLD + AT potentials give accurate prediction of the vapor pressure with an average deviation of 5% from experiment.

C. Surface tension and three-body contributions

The three-body contribution to the surface tension can be derived from the Kirkwood-Buff approach.[42,43] For independent triplets

$$\gamma^{(3\text{B})} = \frac{1}{2A}\left\langle \sum_i \sum_{j>i} \sum_{k>j} \frac{\partial v^{(3\text{B})}}{\partial A} \right\rangle \tag{4}$$

with A the area of the interface. $\partial v^{(3\text{B})}/\partial A$ contains three terms representing the partial derivatives with respect to the three distances in the triplet:

$$\begin{aligned}\frac{\partial v^{(3\text{B})}}{\partial A} = &\frac{\partial v^{(3\text{B})}}{\partial r_{ij}}\left[\frac{r_{ij}^2 - 3z_{ij}^2}{r_{ij}}\right] \\ &+ \frac{\partial v^{(3\text{B})}}{\partial r_{ik}}\left[\frac{r_{ik}^2 - 3z_{ik}^2}{r_{ik}}\right] \\ &+ \frac{\partial v^{(3\text{B})}}{\partial r_{jk}}\left[\frac{r_{jk}^2 - 3z_{jk}^2}{r_{jk}}\right].\end{aligned} \tag{5}$$

The averages of the three terms must be identical by symmetry but we calculate them explicitly in the simulation to improve the statistical accuracy of the averaging. Fig. 4 shows the convergence of $\gamma^{(2\text{B})}$ and $\gamma^{(3\text{B})}$ for the NLD + AT potential at $T = 110$ K during the course of the simulation.

At 110 K in Fig. 4, the standard error in the mean for $\gamma^{(2\text{B})}$ is 0.21 mN m^{-1} and the corresponding standard error in the mean for $\gamma^{(3\text{B})}$ is 0.01 mN m^{-1} in a well converged surface tension with an error bar 3% of the total value. The long-range correction to the two-body contribution is calculated using the Blockhuis[40,41] approach for a single interface. The long-range correction to the three-body contribution of the surface tension is calculated by integrating over all possible atom triplets (i, j, k). In order to considerate those parts of space not covered by Eq. (4) (for which every distance must be $\leq r_c^{3B}$), the long-range correction considers triplets with at least one distance greater than the cutoff radius. For symmetry reasons, we consider only the triplets for which $r_{ij} > r_c^{3B}$ and $r_{ij} > r_{ik} > r_{jk}$ which is one of the six equivalent situations for all

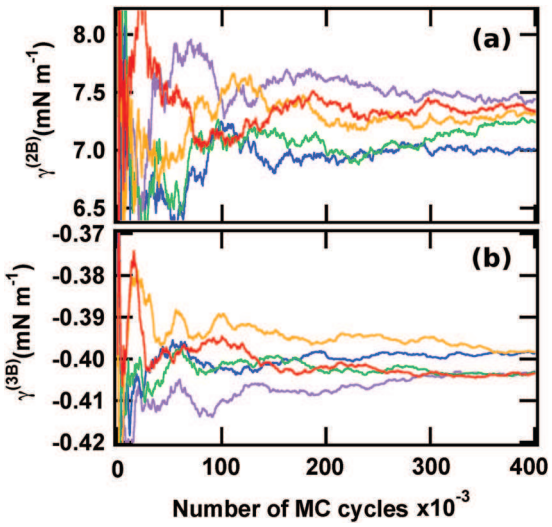

FIG. 4. Evolution of the average value of the surface tension at 110 K using the NDL + AT potential for five independent blocks of 4×10^5 cycles: (a) two-body contribution from Eq. (2); (b) three-body contribution from Eq. (4).

triplets. Using Eq. (5), we obtain

$$\begin{aligned}\gamma_{LRC}^{(3\text{B})} = \frac{1}{6A} \iiint_{r_{ij}>r_c^{(3\text{B})}, r_{ij}>r_{ik}>r_{jk}} &d\mathbf{r}_i d\mathbf{r}_j d\mathbf{r}_k \frac{\partial v^{(3\text{B})}}{\partial A} \\ &\times \rho(z_i)\rho(z_j)\rho(z_k) g^{(2)}(\mathbf{r}_i, \mathbf{r}_k) g^{(2)}(\mathbf{r}_j, \mathbf{r}_k),\end{aligned} \tag{6}$$

where $\rho(z)$ is the single-atom density at z and $g^{(2)}(\mathbf{r}_1, \mathbf{r}_2)$ is the two-body distribution function. We have used the Kirkwood superposition approximation to factorise $\rho^{(3)}(\mathbf{r}_i, \mathbf{r}_j, \mathbf{r}_k)$. Since $r_{ij} > r_c^{(3\text{B})}$, $g^{(2)}(\mathbf{r}_i, \mathbf{r}_j) = 1$.

$g^{(2)}(\mathbf{r}_1, \mathbf{r}_2)$ can be calculated by using a set of internal coordinates for particles 1 and 2 which takes advantage of the cylindrical symmetry of the interface: we have used z_1, $\cos\theta_{12}$ and r_{12} as coordinates to calculate and store $g^{(2)}(z_1, \cos\theta_{12}, r_{12})$ in a three dimensional array. θ_{12} is the angle between $\mathbf{r}_{12}$ and the normal to the surface. Once $g^{(2)}$ is calculated, values for a given pair of atoms are extracted using a trilinear interpolation.

$\gamma_{LRC}^{(3\text{B})}$ is evaluated using a Monte Carlo integration, sampling on a uniform hypercube of side $2r_{\max}$ to obtain a trial point $\{z_i, x_j, y_j, z_j, x_k, y_k, z_k\}$ with $x_i = x_j = 0$. To achieve convergence, we perform the integration using 5×10^{10} trial points and $r_{\max} = 30$ Å. Fluctuations are estimated by averaging 12 integrations performed with different random seeds. The results of the calculation of the four contributions to the surface tension are summarized in Table I. The total values are plotted in Fig. 5 at different temperatures along the coexistence curve.

First, the two-body, effective LJ potential gives values of γ that deviate significantly from experiment with a maximum difference of 33% approaching the critical point. Second, the surface tensions calculated from total potential, the accurate pair potential, and the three-body potential are in better agreement with experiment.

The different contributions to the surface tension are reported in Table I. The short-range part of the two-body contribution $\gamma^{(2\text{B})}$ is identical within the statistical fluctuations for

This article is copyrighted as indicated in the article. Reuse of AIP content is subject to the terms at: http://scitation.aip.org/termsconditions. Downloaded to IP: 194.214.132.176 On: Tue, 01 Jul 2014 07:05:24

TABLE I. Different contributions to the surface tension calculated using three models: a Lennard-Jones truncated (LJT) potential, two potentials including the three-body interactions (BFW + AT), and (NLD + AT). The subscript number indicates the fluctuation on the last digit: -0.41_2 means -0.41 ± 0.02 and 13.58_{16} means 13.58 ± 0.16. Values are in mN m^{-1}. The relative deviations from experimental values are given in percentages.

T	$\gamma^{(2B)}$	$\gamma^{(2B)}_{LRC}$	$\gamma^{(3B)}$	$\gamma^{(3B)}_{LRC}$	γ_{tot}	Deviation (%)
			LJT model			
85	13.86_{33}	1.51			15.37_{33}	+16.7
90	12.52_{17}	1.43			13.94_{18}	+17.2
95	11.20_{18}	1.34			12.54_{19}	+17.5
100	10.16_{21}	1.25			11.41_{22}	+20.6
105	8.89_{13}	1.16			10.05_{14}	+21.2
110	7.51_{18}	1.05			8.57_{19}	+19.8
115	6.54_{19}	0.95			7.48_{20}	+23.6
120	5.33_{13}	0.84			6.17_{13}	+23.4
125	4.31_{9}	0.72			5.03_{10}	+26.1
130	3.38_{9}	0.59			3.98_{10}	+31.2
135	2.40_{11}	0.45			2.85_{11}	+33.3
			BFW + AT			
85	12.67_{28}	0.94	-0.88_{1}	-0.43_{1}	12.30_{36}	− 6.6
90	11.65_{20}	0.88	-0.75_{1}	-0.40_{1}	11.39_{23}	− 4.3
95	10.12_{21}	0.83	-0.67_{1}	-0.37_{2}	9.91_{24}	− 7.1
100	8.96_{26}	0.77	-0.56_{1}	-0.34_{2}	8.83_{29}	− 6.6
105	8.01_{11}	0.71	-0.48_{1}	-0.31_{2}	7.93_{13}	− 4.3
110	6.69_{21}	0.65	-0.40_{1}	-0.27_{1}	6.67_{24}	− 6.8
115	5.53_{13}	0.58	-0.33_{1}	-0.24_{1}	5.54_{16}	− 8.5
120	4.50_{16}	0.50	-0.25_{1}	-0.21_{1}	4.54_{18}	− 9.1
125	3.42_{6}	0.42	-0.19_{1}	-0.17_{1}	3.47_{8}	− 12.9
130	2.42_{10}	0.33	-0.13_{1}	-0.14_{1}	2.48_{11}	− 18.3
135	1.68_{10}	0.24	-0.08_{1}	-0.10_{1}	1.73_{11}	− 18.9
			NLD + AT			
85	13.58_{16}	0.93	-0.86_{1}	-0.42_{2}	13.23_{19}	+0.5
90	12.28_{29}	0.88	-0.75_{1}	-0.41_{2}	12.00_{33}	+0.8
95	11.03_{32}	0.82	-0.65_{1}	-0.37_{2}	10.84_{35}	+1.6
100	9.67_{24}	0.77	-0.56_{1}	-0.34_{2}	9.54_{27}	+0.8
105	8.60_{25}	0.71	-0.48_{1}	-0.31_{1}	8.53_{27}	+2.8
110	7.26_{14}	0.65	-0.40_{1}	-0.28_{1}	7.24_{16}	+1.2
115	6.01_{7}	0.59	-0.33_{1}	-0.25_{1}	6.02_{9}	− 0.6
120	5.12_{22}	0.52	-0.26_{1}	-0.21_{1}	5.16_{23}	+3.2
125	4.00_{4}	0.44	-0.20_{1}	-0.18_{1}	4.06_{5}	+1.7
130	3.03_{12}	0.36	-0.15_{1}	-0.15_{1}	3.09_{13}	+2.0
135	2.05_{18}	0.28	-0.10_{1}	-0.12_{1}	2.11_{19}	− 1.4

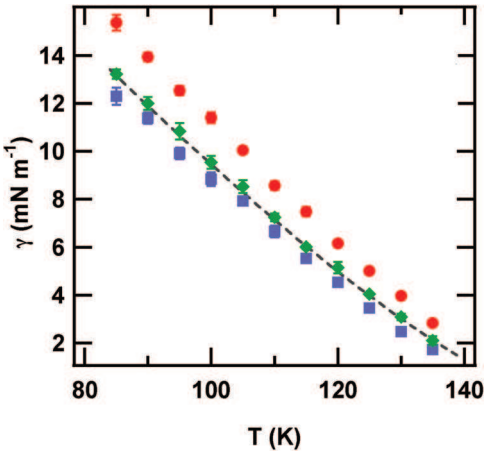

FIG. 5. Surface tension values calculated using • (red) LJ, ■ (blue) (BFW + AT), and ◆ (dark green) (NLD + AT) potentials. The experimental results are shown as the dashed line.[26]

the three potentials. The long-range correction $\gamma^{(2B)}_{LRC}$ is larger for the LJ potential compared with the BFW + AT and the NLD + AT potentials. The three-body contribution to the surface tension is negative, and approximately 6% of the total. $\gamma^{(3B)}_{LRC}$ is the same order of magnitude as the short-range part, at all temperatures. For a triplet of atoms (i, j, k) the short-range part of the three-body potential is only calculated when all three distances are less than $r_c^{(3B)}$. As a consequence, the LRC part, contains triplets with one or more of the separations greater than $r_c^{(3B)}$. This includes triplets containing short distances for which the distribution function $g^{(2)}$ is far from unity regardless of the choice of the cut-off. The three-body LRC must be included in these calculations.

The BFW + AT potential slightly underestimates γ with an average deviation of less than 10%. The deviations from experiments close to the critical temperature can reach as much as 19% which correlates with the poorer prediction of the coexisting density in this region (see Fig. 3). The NLD + AT potential yields the best prediction with a relative deviation of less than 3% over the whole temperature range. This represents a quantitative prediction of the surface tension of argon and confirms the fact that the inclusion of the three-body interaction improves the agreement with experiment.

Other more complete three-body potentials have been developed and used in the simulation of homogeneous fluids.[44] The AT potential is the leading term in these three-body contributions. Since the bare AT contribution brings the simulated γ into agreement with experiment it does no appear to be necessary to include these additional complicated non-additive forms. Since the BFW + AT and NLD + AT potentials use the same potential for the three-body energy, the improved agreement of γ with experiment for NLD + AT model is entirely due to the differences between the two-body potentials. The first derivatives of the NLD and BFW potentials exhibit some small but clear differences in the region 4–7 Å.

IV. CONCLUSIONS

We have simulated an explicit liquid-vapor interface of argon using three-body potentials in order to compare the calculated coexisting densities and surface tension with experiments and reference simulations using an effective two-body potential. We have developed expressions to calculate the three-body contribution to the surface tension and its long-range correction. As the inclusion of the long-range correction to the energy has a large influence on the calculated surface tension in Lennard-Jones fluids, we choose a cutoff value large enough to avoid these cutoff effects. We conclude that the effective Lennard-Jones and the NLD + AT potentials perform very well in the prediction of both coexisting densities and vapor pressures. The extension to the calculation of the surface tension represents then a genuine test of transferability for this potentials.

To do so, we have split the surface tension in four terms: two-body ($\gamma^{(2B)}$), three-body ($\gamma^{(3B)}$), and their long-range corrections. The three-body contribution $\gamma^{(3B)}$ is negative, and converges faster than $\gamma^{(2B)}$ to a stable average value. Additionally, its long-range correction $\gamma^{(3B)}_{LRC}$ appears to be of the

This article is copyrighted as indicated in the article. Reuse of AIP content is subject to the terms at: http://scitation.aip.org/termsconditions. Downloaded to IP: 194.214.132.176 On: Tue, 01 Jul 2014 07:05:24

same order of magnitude than the intrinsic value, because interatomic distances smaller than the cutoff value have to be included in the long-range corrections.

After a careful development of the long-range correction for the three-body term, involving an accurate calculation of the pair distribution function in the interface, and the use of a well-control methodology for the two-phase simulations, we have been able to predict the surface tension for liquid argon along a large part of the orthobaric curve. Some 40 years after the first direct simulations of the surface tension of argon, we have achieved a reconciliation between the simulation and experiment by including the three-body interactions in the simulation.

[1]F. Goujon, P. Malfreyt, A. Boutin, and A. H. Fuchs, Mol. Simul. **27**, 99 (2001).
[2]F. Goujon, P. Malfreyt, A. Boutin, and A. H. Fuchs, J. Chem. Phys. **116**, 8106 (2002).
[3]F. Goujon, P. Malfreyt, J. M. Simon, A. Boutin, B. Rousseau, and A. H. Fuchs, J. Chem. Phys. **121**, 12559 (2004).
[4]C. Ibergay, A. Ghoufi, F. Goujon, P. Ungerer, A. Boutin, B. Rousseau, and P. Malfreyt, Phys. Rev. E **75**, 051602 (2007).
[5]J. Janeček, H. Krienke, and G. Schmeer, Condens. Matter Phys. **10**, 415 (2007).
[6]C. Nieto-Draghi, P. Bonnaud, and P. Ungerer, J. Phys. Chem. C **111**, 15686 (2007).
[7]F. Biscay, A. Ghoufi, F. Goujon, V. Lachet, and P. Malfreyt, J. Phys. Chem. B **112**, 13885 (2008).
[8]F. Biscay, A. Ghoufi, V. Lachet, and P. Malfreyt, Phys. Chem. Chem. Phys. **111**, 6132 (2009).
[9]F. Biscay, A. Ghoufi, and P. Malfreyt, J. Chem. Phys. **134**, 044709 (2011).
[10]F. Biscay, A. Ghoufi, V. Lachet, and P. Malfreyt, J. Phys. Chem. C **115**, 8670 (2011).
[11]N. Ferrando, V. Lachet, J. Pérez-Pellitero, A. D. Mackie, P. Malfreyt, and A. Boutin, J. Phys. Chem. B **115**, 10654 (2011).
[12]R. A. Zubillaga, A. Labastida, B. Cruz, J. C. Martinez, E. Sanchez, and J. Alejandre, J. Chem. Theory Comput. **9**, 1611 (2013).
[13]C. Vega and E. de Miguel, J. Chem. Phys. **126**, 154707 (2007).
[14]A. Ghoufi, F. Goujon, V. Lachet, and P. Malfreyt, J. Chem. Phys. **128**, 154716 (2008).
[15]A. Ghoufi and P. Malfreyt, Phys. Rev. E **83**, 051601 (2011).
[16]J. Alejandre, D. J. Tildesley, and G. A. Chapela, J. Chem. Phys. **102**, 4574 (1995).
[17]A. Ghoufi, F. Goujon, V. Lachet, and P. Malfreyt, Phys. Rev. E **77**, 031601 (2008).
[18]A. Ghoufi, F. Goujon, V. Lachet, and P. Malfreyt, J. Chem. Phys. **128**, 154718 (2008).
[19]J. C. Neyt, A. Wender, V. Lachet, and P. Malfreyt, J. Phys. Chem. B **115**, 9421 (2011).
[20]J. K. Lee, J. A. Barker, and G. M. Pound, J. Chem. Phys. **60**, 1976 (1974).
[21]S. Werth, S. V. Lishchuk, M. Horsch, and H. Hasse, Phys. A **392**, 2359 (2013).
[22]J. Vrabec, G. K. Kedia, G. Fuchs, and H. Hasse, Mol. Phys. **104**, 1509 (2006).
[23]J. Anta, E. Lomba, and M. Lombardero, Phys. Rev. E **55**, 2707 (1997).
[24]G. Marcelli and R. Sadus, J. Chem. Phys. **111**, 1533 (1999).
[25]G. Marcelli and R. Sadus, J. Chem. Phys. **112**, 6382 (2000).
[26]E. W. Lemmon, M. O. McLinden, and D. G. Friend, "Thermophysical properties of fluid systems," in *NIST Chemistry Webbook*, NIST Standard Reference Database Number 69, edited by P. J. Linstrom and W. G. Mallard (National Institute of Standards and Technology, Gaithersburg, MD, 2005), see http://webbook.nist.gov (accessed 5 February 2014).
[27]J. Barker, R. Fischer, and R. Watts, Mol. Phys. **21**, 657 (1971).
[28]R. Sadus and J. Prausnitz, J. Chem. Phys. **104**, 4784 (1996).
[29]D. Zhou, M. Mi, and C. Zhong, J. Phys. Chem. B **115**, 57 (2011).
[30]J. Vrabec, J. Stoll, and H. Hasse, J. Phys. Chem. B **105**, 12126 (2001).
[31]A. Nasrabad, R. Laghaei, and U. Deiters, J. Chem. Phys. **121**, 6423 (2004).
[32]B. Axilrod and E. Teller, J. Chem. Phys. **11**, 299 (1943).
[33]J. G. Kirkwood and F. P. Buff, J. Chem. Phys. **17**, 338 (1949).
[34]J. P. R. B. Walton, D. J. Tildesley, J. S. Rowlinson, and J. R. Henderson, Mol. Phys. **48**, 1357 (1983).
[35]D. Green, G. Jackson, E. de Miguel, and L. Rull, J. Chem. Phys. **101**, 3190 (1994).
[36]F. Biscay, A. Ghoufi, F. Goujon, V. Lachet, and P. Malfreyt, J. Chem. Phys. **130**, 184710 (2009).
[37]M. Guo and B. C. Y. Lu, J. Chem. Phys. **106**, 3688 (1997).
[38]J. Janecek, J. Phys. Chem. B **110**, 6264 (2006).
[39]L. MacDowell and F. Blas, J. Chem. Phys. **131**, 074705 (2009).
[40]G. A. Chapela, G. Saville, S. M. Thompson, and J. S. Rowlinson, J. Chem. Soc., Faraday Trans. **73**, 1133 (1977).
[41]E. M. Blokhuis, D. Bedeaux, C. D. Holcomb, and J. A. Zollweg, Mol. Phys. **85**, 665 (1995).
[42]S. Toxvaerd, Prog. Surf. Sci. **3**, 189 (1972).
[43]M. Grant and R. C. Desai, J. Chem. Phys. **72**, 1482 (1980).
[44]R. Bukowski and K. Szalewicz, J. Chem. Phys **114**, 9518 (2001).

This article is copyrighted as indicated in the article. Reuse of AIP content is subject to the terms at: http://scitation.aip.org/termsconditions. Downloaded to IP: 194.214.132.176 On: Tue, 01 Jul 2014 07:05:24